ORIGINAL RESEARCH ARTICLE

The Effect of *p*-Doped AlInN Last Quantum Barrier on Carrier Concentration of 266 nm Light-Emitting Diodes Without Electron Blocking Layer

Muhammad Usman[1] · **Tariq Jamil**[1]

Abstract

In deep ultraviolet light-emitting diodes (DUV LEDs), we numerically investigate the effect of *p*-doped AlInN last quantum barrier (LQB). The *p*-doped AlInN LQB not only suppresses the electron overflow but also facilitates hole transport. This is attributed to the decreased lattice mismatching between epilayers, i.e., LQB and *p*-AlGaN. Our proposed *p*-doped AlInN LQB LED shows reduced efficiency droop at 200 A/cm^2. Additionally, the peak emission spectra (at 266 nm) of *p*-doped AlInN LQB LED are enhanced by almost twice that of the conventional LED. Our proposed LED has no electron blocking layer (EBL) because the *p*-doped AlInN LQB serves two purposes, i.e., as both LQB and effective EBL.

Keywords AlInN · internal quantum efficiency · deep ultraviolet · light-emitting diodes

Introduction

Contamination-free AlGaN-based deep ultraviolet light-emitting diodes (DUV LEDs) have replaced mercury-based UV lamps and lead-based DUV lamps.[1,2] UV LEDs face performance challenges due to high threading dislocation density (TDD)[3] which originates from mismatching of epilayers.[4] To minimize this, many groups reported different approaches, such as low TDD based on ammonia pulse-flow multilayer.[5] Auger recombination and asymmetric carrier concentration causes severe efficiency droop, which further degrades the optoelectronic performance of UV LEDs.[6] Theoretical models of the efficiency droop mechanism and the effect of the Auger coefficient on the efficiency droop have also been reported.[7,8] Electrons having higher thermal velocity due to their lower effective mass than holes overcome the potential barrier height of quantum barriers (QBs) and electron blocking layer (EBL) and leak into *p*-layers.[3,4] The leaked electron recombines with holes in the *p*-layers leading to non-radiative recombination instead

of a radiative recombination rate.[4] To overcome the electron leakage, many researchers have proposed engineered ternary aluminum gallium nitride (AlGaN) and quaternary aluminum indium gallium nitride (AlInGaN) quantum wells (QWs), QBs, and EBL.[9–11] In addition to electron overflow, hindrance in hole transport in high-aluminum AlGaN layers is a big challenge.[12] Besides higher effective mass of holes, magnesium-dopant (Mg-dopant) activation energy increases with increasing aluminum content.[3,4,13,14] Thus, unwanted asymmetric distribution of electrons/holes is created in the active region.[4,6] The polarization field at the interfaces between epilayers on the *p*-side also hinders hole transport.[13,15] Graded aluminum nitride AlN EBL has been reported to decrease the large induced-polarization field.[16] Other research groups have reported improvement in the carrier concentrations in the active zone with different design approaches.[17,18] Despite these improvements, carrier leakage is still a challenge in the development of efficient DUV LEDs.[18]

Aluminum indium nitride (AlInN) is a promising III-nitride alloy due to its reasonable lattice matching with the rest of the epilayers[19] and, thus, appropriate conduction and valence band offsets.[3] The lattice matching decreases the induced polarization field, which facilitates the transport of holes into the active region.[15,20] Moreover, the higher conduction band offset is favorable for the suppression of electron leakage.[10] Therefore, in many recent reports, AlInN

✉ Muhammad Usman
usmanishfaq@yahoo.com

1 Faculty of Engineering Sciences, Ghulam Ishaq Khan Institute of Engineering Sciences and Technology, Topi 23460, Khyber Pakhtunkhwa, Pakistan

alloy has been used both experimentally and theoretically for the development of efficient UV LEDs.[20–22] Inspired by these features, we studied the influence of *p*-doped AlInN LQB LED structure without EBL on carrier optimization numerically in this work. Recently, DUV LED without EBL has been reported where graded Al composition for all QBs has been employed.[23] Stri*p*-in-barrier structure without EBL has been reported in nanowire DUV LED.[24] In this work, we employ *p*-AlInN LQB and analyze its influence on the carrier leakage in an EBL-free DUV LED (with a peak emission wavelength of 266 nm). According to our results, both concentrations of electrons and holes in the active region of the proposed *p*-AlInN LQB LED are enhanced simultaneously. Thus, the optoelectronic performance of *p*-doped AlInN LED is improved markedly. Importantly, the *p*-AlInN serves as both LQB and EBL , eliminating the need for a typical AlGaN EBL. It may be noted that many researchers have demonstrated good-quality AlInN layer.[19,22]

Device Structures and Parameters

Figure 1a illustrates the structure of a conventional LED. The electron injector layer n-$Al_{0.68}Ga_{0.32}$ N was grown on a sapphire substrate, silicon-doped (Si-doped) at a concentration of 1×10^{17} cm^{-3}. The active zone comprises five pairs of QWs/QBs, i.e., $Al_{0.52}Ga_{0.48}$ N/$Al_{0.58}Ga_{0.42}$ N. The wavelength of emitted photons is ∼ 266 nm, which lies in the DUV range, an important wavelength for sterilization, sensing, and air/water purification. The widths of the QW and QB are 2 nm and 12 nm, respectively. Ten-nanometer-wide *p*-EBL ($Al_{0.65}Ga_{0.35}$ N) with Mg

concentration of 1×10^{20} cm^{-3} is used. The hole reservoir layer, i.e., *p*-$Al_{0.55}Ga_{0.45}$ N and *p*-contact layer GaN (each 100 nm thick) are grown on *p*-EBL, respectively. Both the layers are *p*-doped with Mg concentration of 1×10^{19} cm^{-3}. Figure 1b shows the energy band schematic of the electron injector layer, last quantum well (LQW), QBs, EBL, and hole injector layer. The mechanism of electron leakage, hole transport, and radiative recombination is shown in the figure. In all LEDs, the encircled conduction band part in Fig. 1b shows the trapping of electrons. In the valence band, the encircled part shows holes being trapped. LED NI is a conventional LED. In LED NII, we introduced *p*-$Al_{0.65}Ga_{0.35}$ N LQB (with Mg concentration of 1×10^{20} cm^{-3}) instead of conventional undoped $Al_{0.58}Ga_{0.42}$ N LQB. In LED NIII, the *p*-AlGaN LQB of LED NII is replaced by the *p*-$Al_{0.96}In_{0.04}$ N layer with the same Mg concentration: 1×10^{20} cm^{-3}. Notably, the size of the LQB (12 nm) is the same for all LEDs. LED NII and LED NIII are without conventional *p*-AlGaN EBL. All the LED chips are in the size of 300×300 um^2. The conduction/valence band offset is 0.7/0.3.[25] The Shockley–Read–Hall (SRH) recombination coefficient life span is 10 ns, while the Auger coefficient value is 2.88×10^{-30} cm^6/s. The screening factor is 40%, which is in the typical reported range[26] while the operating temperature for all structures is 300 K. The electron and hole mobilities are 100 cm^2/V.s and 10 cm^2/V.s, respectively. Keeping all the operational parameters the same, we determine the influence of *p*-doped $Al_{0.96}In_{0.04}$ N LQB in this study. We study the optoelectronic characteristics including internal quantum efficiency (IQE), emission spectra, and current–voltage (*I–V*) of our devices. All LED devices are numerically
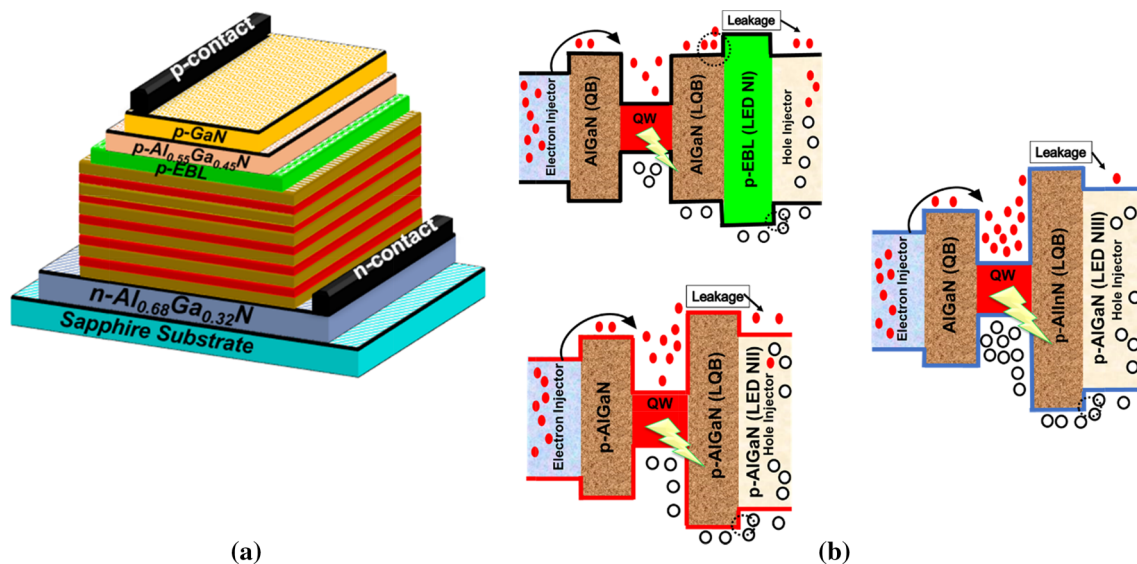

Fig. 1 (a) Conventional LED structure, (b) band illustration of the electron injector layer, LQW, and LQB layer, *p*-EBL layers, and hole injector layer, denoted by LED NI, NII, and NIII.

simulated by SiLENSe™ 6.3. The simulation tool and the remaining parameters are according to the reference.[26,27]

Results and Discussion

Figure 2 presents the band diagram of all LEDs at 80 A/cm². The φ_e (effective potential conduction barrier height) and φ_h (effective potential valence barrier height) in LED NI are 333 meV and 345 meV, respectively. φ_e in LED NII is increased from 333 to 359 meV. Conversely, φ_h in LED NII is decreased from 345 to 315 meV, as shown in Fig. 2b. Hence, the LED NII suppresses the electron leakage and facilitates hole transport more effectively than LED NI. Similarly, φ_e in LED NIII is increased from 359 to 428 meV while φ_h is decreased from 315 to 301 meV in Fig. 2c. Thus, LED NIII not only confines electrons but also facilitates hole transport more effectively than LED NII. Employing AlInN LQB decreased the lattice mismatch between AlGaN QB

and p-AlGaN EBL epilayers.[20] Additionally, the removal of p-AlGaN EBL mitigates the band bending in LED NII and LED NIII. The band bending between the epilayers accumulates electrons and holes, leading to non-radiative recombination.[10,24]

We computed the carrier concentration profile for all LEDs, as illustrated in Fig. 3. It can be noted that a 2.5 nm x-axis shift (towards p-side) in Fig. 3 is done to avoid the overlapping of results and clarity for the audience. The electron concentration in LED NII and LED NIII is clearly greater than that in LED NI in Fig. 3a. The electron concentration in LED NII and LED NIII is improved by 14% and 36%, respectively, compared with LED NI. Higher φ_e suppresses the electron leakage to p-layers. Moreover, the band bending at the LQB and EBL interface is mitigated in LED NII and LED NIII, where electron are wasted.[10] Meanwhile, the hole concentration in the LED NII and LED NIII is also enhanced, as presented in Fig. 3b. The hole concentration in LED NII and LED NIII increased by 7% and 24%,
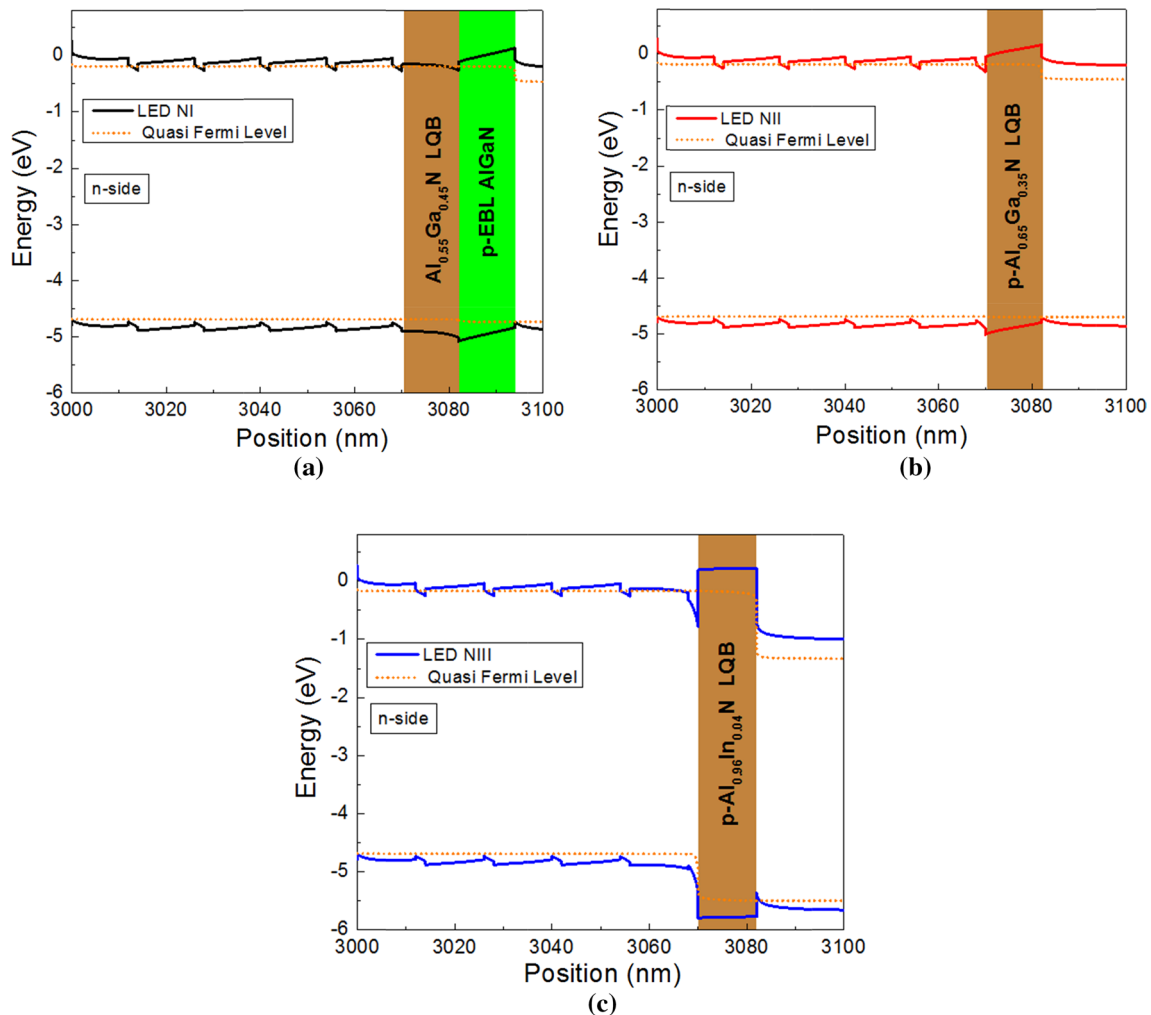

Fig. 2 Energy band profile of (a) LED NI, (b) LED NII, and (c) LED NIII at 80 A/cm².

respectively, as compared with LED NI. In LED NII, the increase in φ_e is due to the increase in Al concentration in LQB. Thus, *p*-Al$_{0.65}$Ga$_{0.35}$N LQB suppresses the electron leakage but disrupts the transport of holes in LED NII as compared with LED NIII due to increased lattice mismatching.[15] The remarkable holes improvement in LED NIII is due to the lower φ_h resulting from lattice matching of epilayers, which facilitates the highest hole transport to the active region among other LEDs.[15,20] Both the electron and hole concentrations in LED NIII are increased by 19% and 16% as compared with LED NII.

In Fig. 4a, the electron leakage in LED NII and LED NIII is decreased effectively. The leakage in LED NIII is negligible as compared with the other two LEDs, which is attributed to higher φ_e in LED NIII. Interestingly, the holes entrance in LED NII and LED NIII is also enhanced in Fig. 4b. In LED NII and LED NIII, it is increased by 1.40

and 1.65 times, respectively, as compared to LED NI. Importantly, the entrance of the hole into the active region of LED NIII is 1.18 times greater than that in LED NII.

Comparatively high radiative recombination rates of 50% and 119% are observed in LED NII and LED NIII, respectively, as compared with LED NI in Fig. 5a. It can be seen that a 2.5 nm *x*-axis shift (towards *p*-side) in Fig. 5a is done to avoid the overlapping of results and clarity for the audience The higher radiative recombination rate results in higher photon extraction, leading to higher IQE, which is the main parameter for the scaling of optical performance in any optoelectronic device.[4] Figure 5b shows the calculated IQE for all LEDs. The peak values of IQE for LED NI, LED NII, and LED NIII are 34%, 47%, and 56%, respectively. The IQE in LED NII and LED NIII is increased by 38% and 65%, respectively. Moreover, the efficiency droop in LED NI, LED NII, and LED NIII is 21%, 4%, and nearly 0% at
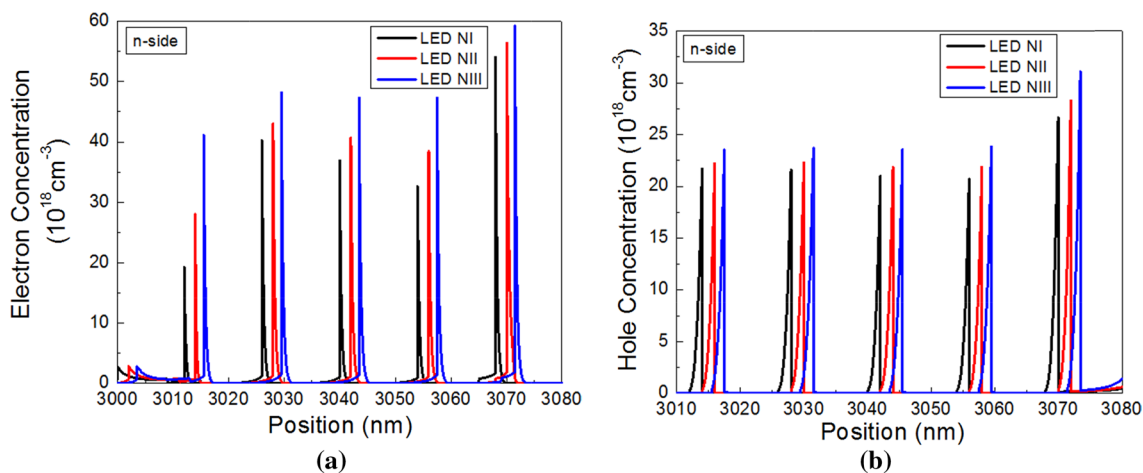

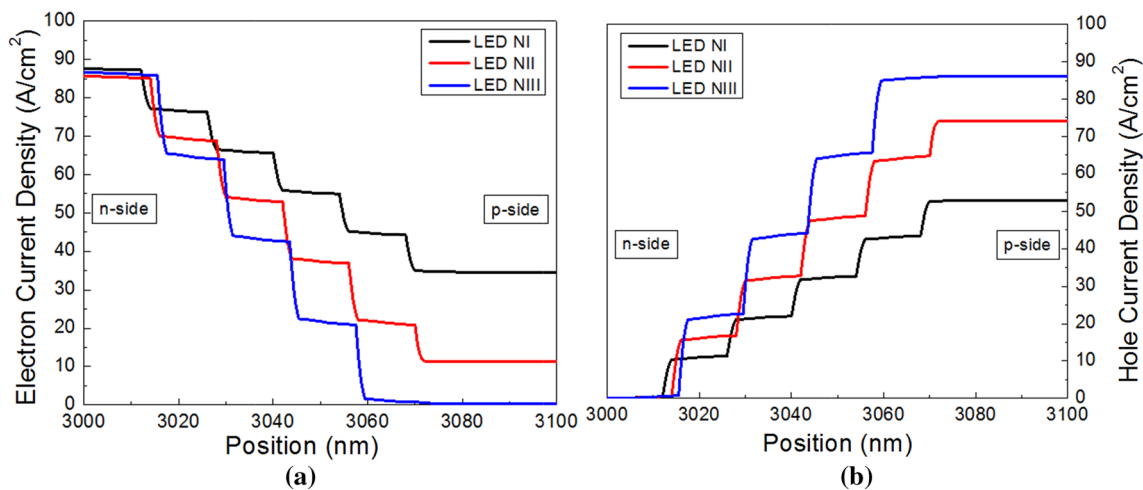**Fig. 3** At 80 A/cm^2 carrier concentration in the QWs: (a) Electron, (b) Hole.

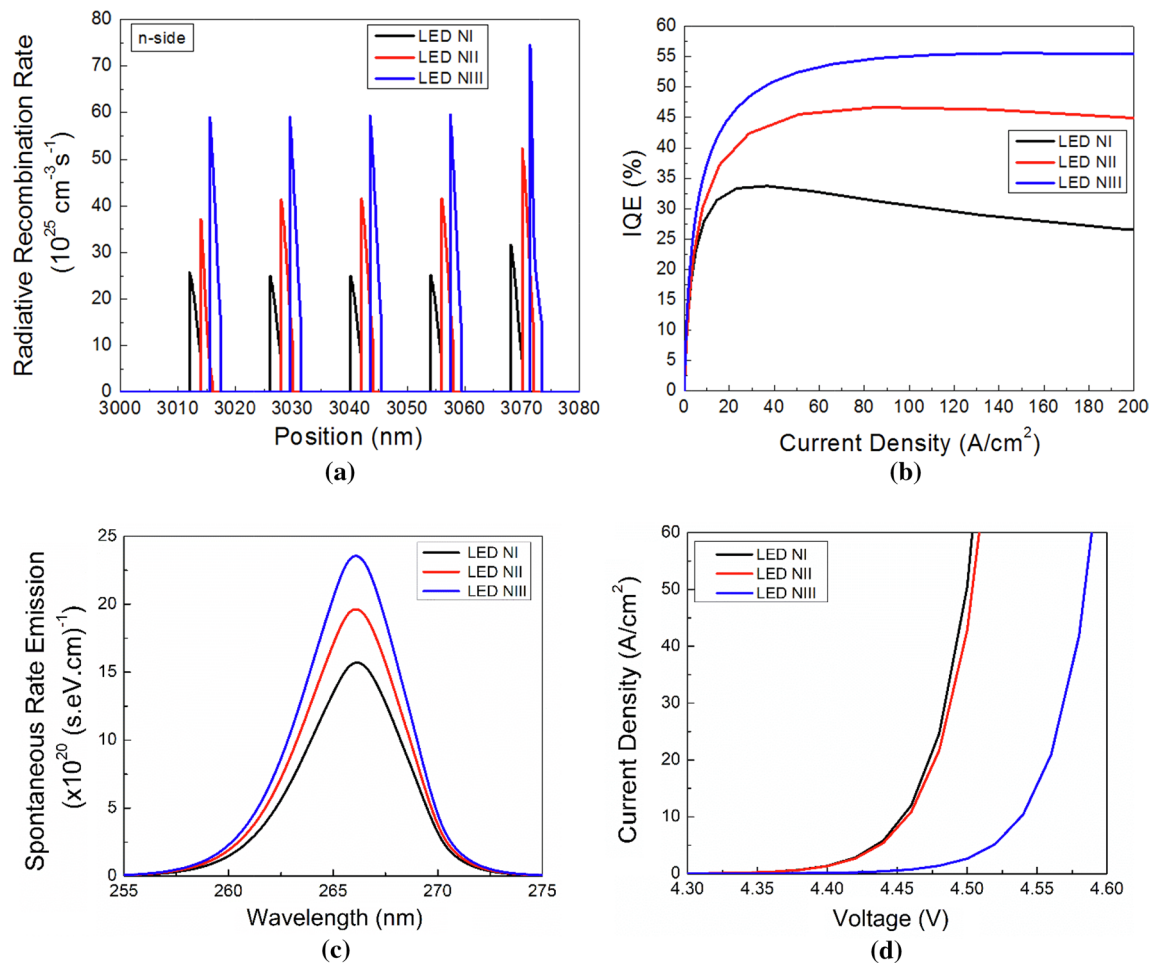**Fig. 4** Carrier flux: (a) electrons, (b) holes at 80 A/cm^2.

Fig. 5 (a) Radiative recombination rate, (b) IQE, (c) emission, (d) current–voltage of LED NI, LED NII, and LED NIII.

200 A/cm^2. Figure 5c shows emission intensity at 80 A/cm^2. The peak wavelength of all LEDs is observed at ∼ 266 nm. It can be concluded that the *p*-AlInN layer does not influence the peak emission wavelength. The emission spectra of LED NII and LED NIII are enhanced two- and threefold, respectively, as compared with LED NI. Figure 5d illustrates the *I–V* characteristics of all LEDs. Higher forward voltage is observed for LED NIII than for the other two LEDs. The increased turn-on voltage can be attributed to the high aluminum content in LED NIII.

Conclusion

This study reports the numerical investigation of *p*-doped AlInN LQB DUV LED. We proposed a DUV LED with *p*-doped AlInN LQB (without conventional *p*-AlGaN EBL). Our results show that *p*-AlInN LQB facilitates hole

transport and suppresses electron leakage. The higher conduction band offset and lower valence band offset with the use of *p*-doped AlInN LQB are the reason behind this improvement in our DUV LED. The improved band offsets are further attributed to lower lattice mismatching between AlGaN LQB and *p*-AlGaN EBL epilayers. The radiative recombination rate and IQE are improved by 119% and 65% in LED NIII, respectively, as compared with the conventional LED. The *p*-doped AlInN LQB also worked as an alternative yet effective EBL for high-IQE UV LEDs.

References

1. Y. Muramoto, M. Kimura, and S. Nouda, Development and Future of Ultraviolet Light-Emitting Diodes: UV-LED will Replace the UV Lamp. *Semicond. Sci. Technol.* 29, 084004 (2014).

2. E.F. Schubert and J.K. Kim, Solid-State Light Sources Getting Smart. *Science* 308, 1274 (2005).

3. H. Morkoç: *Handbook of Nitride Semiconductors and Devices, MATERIALS Properties, Physics and Growth.* (John Wiley and Sons, 2009).

4. S. M. Sze, Y. Li and K. K. Ng: *Physics of Semiconductor Devices.* (John Wiley and Sons, 2021).

5. H. Hirayama, S. Fujikawa, N. Noguchi, J. Norimatsu, T. Takano, K. Tsubaki, and N. Kamata, 222–282 nm AlGaN and InAlGaN-based Deep-UV LEDs Fabricated on High-Quality AlN on Sapphire. *Phys. Status Solidi (a)* 206, 1176 (2009).

6. J. Cho, E.F. Schubert, and J.K. Kim, Efficiency Droop in Light-Emitting Diodes: Challenges and Countermeasures. *Laser Photonics Rev.* 7, 408 (2013).

7. J. Piprek, Efficiency Droop in Nitride-Based Light-Emitting Diodes. *Phys. Status Solidi (a)* 207, 2217 (2010).

8. E. Kioupakis, Q. Yan, and C.G. Van de Walle, Interplay of Polarization Fields and Auger Recombination in the Efficiency Droop of Nitride Light-Emitting Diodes. *Appl. Phys. Lett.* 101, 231107 (2012).

9. J.-Y. Chang, M.-F. Huang, F.-M. Chen, B.-T. Liou, Y.-H. Shih, and Y.-K. Kuo, Effects of Quantum Barriers and Electron-Blocking Layer in Deep-Ultraviolet Light-Emitting Diodes. *J. Phys. D Appl. Phys.* 51, 075106 (2018).

10. Z. Ren, H. Yu, Z. Liu, D. Wang, C. Xing, H. Zhang, C. Huang, S. Long, and H. Sun, Band Engineering of III-Nitride-based Deep-Ultraviolet Light-Emitting Diodes: A Review. *J. Phys. D Appl. Phys.* 53, 073002 (2019).

11. M. Usman, T. Jamil, S. Malik, and H. Jamal, Designing Anti-Trapezoidal Electron Blocking Layer for the Amelioration of AlGaN-based Deep Ultraviolet Light-Emitting Diodes Internal Quantum Efficiency. *Optik* 232, 166528 (2021).

12. Y.-K. Kuo, J.-Y. Chang, F.-M. Chen, Y.-H. Shih, and H.-T. Chang, Numerical Investigation on the Carrier Transport Characteristics Of AlGaN dee*p*-UV Light-Emitting Diodes. *IEEE J. Quantum Electron.* 52, 1 (2016).

13. J. Simon, V. Protasenko, C. Lian, H. Xing, and D. Jena, Polarization-Induced Hole Doping in Wide–Band-Gap Uniaxial Semiconductor Heterostructures. *Science* 327, 60 (2010).

14. T. Kinoshita, T. Obata, H. Yanagi, and S.-I. Inoue, High *p*-Type Conduction in High-Al Content Mg-doped AlGaN. *Appl. Phys. Lett.* 102, 012105 (2013).

15. Y.-K. Kuo, J.-Y. Chang, H.-T. Chang, F.-M. Chen, Y.-H. Shih, and B.-T. Liou, Polarization Effect in AlGaN-Based Deep-Ultraviolet Light-Emitting Diodes. *IEEE J. Quantum Electron.* 53, 1 (2016).

16. Z.-H. Zhang, J. Kou, S.-W.H. Chen, H. Shao, J. Che, C. Chu, K. Tian, Y. Zhang, W. Bi, and H.-C. Kuo, Increasing the Hole Energy by Grading the Alloy Composition of the *p*-Type Electron Blocking Layer for Very High-Performance Deep Ultraviolet Light-Emitting Diodes. *Photonics Res.* 7, B1 (2019).

17. M. Usman, S. Malik, M.A. Khan, and H. Hirayama, Suppressing the Efficiency Droop in AlGaN-based UVB LEDs. *Nanotechnology* 32, 215703 (2021).

18. M. Kneissl, T.-Y. Seong, J. Han, and H. Amano, The Emergence and Prospects of Deep-Ultraviolet Light-Emitting Diode Technologies. *Nat. Photonics* 13, 233 (2019).

19. D. Borovac, W. Sun, R. Song, J.J. Wierer Jr., and N. Tansu, On the Thermal Stability of Nearly Lattice-Matched AlInN Films Grown on GaN via MOVPE. *J. Cryst. Growth* 533, 125469 (2020).

20. J. Huang, Z. Guo, M. Guo, Y. Liu, S. Yao, J. Sun, and H. Sun, Study of Deep Ultraviolet Light-Emitting Diodes with ap-AlInN/AlGaN Superlattice Electron-Blocking Layer. *J. Electron. Mater.* 46, 4527 (2017).

21. R.B. Chung, C. Han, C.-C. Pan, N. Pfaff, J.S. Speck, S.P. DenBaars, and S. Nakamura, The Reduction of Efficiency Droop by $Al_{0.82}In_{0.18}N$/GaN Superlattice Electron Blocking Layer in (0001) Oriented GaN-Based Light Emitting Diodes. *Appl. Phys. Lett.* 101, 131113 (2012).

22. R.T. Velpula, B. Jain, M.R. Philip, H.D. Nguyen, R. Wang, and H.P.T. Nguyen, Epitaxial Growth and Characterization of AlInn-Based Core-Shell Nanowire Light Emitting Diodes Operating in the Ultraviolet Spectrum. *Sci. Rep.* 10, 1 (2020).

23. Z. Ren, Y. Lu, H.-H. Yao, H. Sun, C.-H. Liao, J. Dai, C. Chen, J.-H. Ryou, J. Yan, and J. Wang, III-Nitride Deep UV LED Without Electron Blocking Layer. *IEEE Photonics J.* 11, 1 (2019).

24. R.T. Velpula, B. Jain, H.Q.T. Bui, T.T. Pham, H.-D. Nguyen, T.R. Lenka, and H.P.T. Nguyen, Numerical Investigation On the Device Performance of Electron Blocking Layer Free AlInN Nanowire Deep Ultraviolet Light-Emitting Diodes. *Optical Materials Express* 10, 472 (2020).

25. C. Coughlan, S. Schulz, M.A. Caro, and E.P. O'Reilly, Band gap Bowing and Optical Polarization Switching in Al Ga N Alloys. *Phys. Status Solidi (b)* 252, 879 (2015).

26. J. Yun, J.-I. Shim, and H. Hirayama, Analysis of Efficiency Droop in 280-nm AlGaN Multiple-Quantum-Well Light-Emitting Diodes Based on Carrier Rate Equation. *Appl. Phys. Express* 8, 022104 (2015).

27. SiLENSETM by STR Group Russia, Online: https://www.str-soft.com/devices/silense/ Access Date 01 July 2022.